Photoinduced three-dimensional orientational order in side chain liquid crystalline azopolymers

O. V. Yaroshchuk,[1,*] A. D. Kiselev,[2,†] Yu. Zakrevskyy,[1] T. Bidna,[1] J. Kelly,[3] L.-C. Chien,[3] and J. Lindau[4]
[1]*Institute of Physics of NASU, prospekt Nauki 46, 03028 Kyïv, Ukraine*
[2]*Chernigov State Technological University, Shevchenko Street 95, 14027 Chernigov, Ukraine*
[3]*Kent State University, Liquid Crystal Institute, Kent, Ohio 44242, USA*
[4]*Institute of Physical Chemistry, Martin-Luther University, Mühlphorte 1, 06106 Halle, Germany*
(Received 25 March 2003; published 24 July 2003)

We apply experimental technique based on the combination of methods dealing with principal refractive indices and absorption coefficients to study the photoinduced three-dimensional (3D) orientational order in the films of liquid crystalline (LC) azopolymers. The technique is used to identify 3D orientational configurations of *trans* azobenzene chromophores and to characterize the degree of ordering in terms of order parameters. We study two types of LC azopolymers which form structures with preferred in-plane and out-of-plane alignment of azochromophores, respectively. Using irradiation with the polarized light of two different wavelengths, we find that the kinetics of photoinduced anisotropy can be dominated by either photoreorientation (angular redistribution of *trans* chromophores) or photoselection (angular selective *trans-cis* isomerization) mechanisms depending on the wavelength. At the early stages of irradiation, the films of both azopolymers are biaxial. This biaxiality disappears on reaching a state of photosaturation. In the regime of photoselection, the photosaturated state of the film is optically isotropic. But, in the case of the photoreorientation mechanism, anisotropy of this state is uniaxial with the optical axis dependent on the preferential alignment of azochromophores. We formulate the phenomenological model describing the kinetics of photoinduced anisotropy in terms of the isomer concentrations and the order parameter tensor. We present the numerical results for absorption coefficients that are found to be in good agreement with the experimental data. The model is also used to interpret the effect of changing the mechanism with the wavelength of the pumping light.

DOI: 10.1103/PhysRevE.68.011803 PACS number(s): 61.30.Gd, 78.66.Qn

I. INTRODUCTION

Azobenzene and its derivatives have attracted much attention over the past few decades because of a number of fascinating features of these compounds. They were initially used in preparation of paints, because of rich spectrum of colors that can be obtained depending on the chemical structure of azochromophores. Further investigations revealed strong photochromism (photomodification of color) of azobenzene derivatives. It was found that this effect in azobenzene derivatives can be accompanied by a novel phenomenon that is known as photoinduced optical anisotropy (POA) and can be detected in dichroism and birefringence measurements [1].

The discovery of POA opened up a new chapter in the studies of azobenzene compounds. Neporent and Stolbova [2] described POA in viscous solutions of azodyes, then Todorov and co-workers [3] disclosed the same phenomenon in azodye-polymer blends. The anisotropy induced in these systems is rather unstable. The stable POA was observed later on in polymers containing chemically linked azochromophores (azopolymers) [4]. It turned out that stable anisotropy can be induced in both amorphous and liquid crystalline (LC) azopolymers [4–10]. The efficiency of POA in LC azopolymers is generally much higher than it is for amorphous homologs. For example, the photoinduced birefringence can be as high as 0.3 [10] that is a typical value for low-molecular-weight LCs [11].

It is commonly accepted that the macroscopic anisotropy detected in optical experiments reflects the microscopic orientational order of polymer fragments which is mainly determined by the order of azochromophores in *trans* configuration. There are two known phenomena underlying the process of orientational ordering of the azochromophores: (a) strong absorption dichroism of azobenzene groups that have the optical transition dipole moment approximately directed along the long molecular axis; (b) photochemically induced *trans-cis* isomerization and subsequent thermal and/or photochemical *cis-trans* back isomerization of azobenzene moieties.

It means that the rate of the photoinduced isomerization strongly depends on orientation of the azobenzene chromophores relative to the polarization vector of actinic light **E**. The fragments oriented perpendicular to **E** are almost inactive, whereas the groups with the long axes parallel to **E** are the most active for isomerization.

There are two different regimes of the photoinduced ordering. These regimes are usually recognized as two limiting cases related to the lifetime of *cis* isomers under irradiation, and were theoretically considered in Refs. [12,13].

If *cis* isomers are long living, the anisotropy is caused by angular selective burning of mesogenic *trans* isomers due to stimulated transitions to nonmesogenic *cis* form. The transition rate is angular dependent, so that the *trans* azochromophores normally oriented to **E** are the least burned. This direction will define the axis of the induced anisotropy. This regime of POA is known as the mechanism of angular hole burning (photoselection).

*Email address: olegyar@iop.kiev.ua
†Email address: kisel@elit.chernigov.ua

In the opposite case of short-living *cis* isomers, the azochromophores are excited many times during the POA generation period. These *trans-cis-trans* isomerization cycles are accompanied by rotations of the azochromophores that tend to assume orientation transverse to **E** and minimize the absorption. Nonphotosensitive groups can be involved in the process of reorientation due to cooperative motion [6,14]. This regime is referred to as the photoreorientation (angular redistribution) mechanism.

From the above it might be concluded that, whichever mechanism of the ordering is assumed, the exciting light causes preferential alignment of azobenzene chromophores along the directions perpendicular to the polarization vector of the actinic light. In three-dimensional (3D) space, these directions form the plane normal to **E**. It can be expected that the angular distribution of azochromophores in this plane is isotropic. From the experimental results, however, this is not the case. The uniaxial ordering with strongly preferred in-plane alignment was observed in Refs. [10,15]. In addition, it was found that the photoinduced orientational structures can show biaxiality [8,10,16–18].

This implies that actually the system is not spherically symmetric in the absence of light and some of the above directions are preferred depending on a number of additional factors such as irradiation conditions, chemical structure of polymers, surface interaction, etc. These factors combined with the action of light may result in a large variety of orientational configurations (uniaxial, biaxial, splayed) characterized by different spatial orientations of the principal axes.

In the past years, this spatial character of the photoinduced anisotropies has not received much attention and, until recently, it has been neglected in the bulk of experimental and theoretical studies of POA in azobenzene containing polymers [4,12–14,19–24]. On the other hand, the problems related to the 3D orientational structures in polymeric films are currently of considerable importance in the development of new compensation films for liquid crystal displays [25] and the pretilt angle generation by the use of photoalignment method of LC orientation [26].

The known methods suitable for the experimental study of the 3D orientational distributions in polymer films can be divided into two groups.

The methods of the first group are based on absorption measurements. These methods have the indisputable advantage that the order parameters of various molecular groups can be estimated from the results of these measurements. Shortcomings of the known absorption methods [8,27] are the limited field of applications and the strong approximations.

The second group includes the methods dealing with principal refractive indices. Recently, several variations of the prism coupling methods have been applied to measure the principal refractive indices in azopolymer films [28–30]. These results, however, were not used for in-depth analysis of such features of the spatial ordering as biaxiality and spatial orientation of the optical axes depending on polymer chemical structure, irradiation conditions, etc.

Our goal is a comprehensive investigation of the peculiarities of 3D orientational ordering in azopolymers.

In our previous studies [10,15,18], we were mainly concerned with the effects related to the peculiarities of azopolymer self-organization, which, in addition to the symmetry axis defined by the light polarization, affect the light-induced 3D ordering. The combination of methods described in Ref. [18] was found to be an experimental technique particularly suitable to characterize light-induced anisotropy of orientational structures in azopolymer films. We have investigated these structures depending on the polarization state of the actinic light [10] and on the molecular constitution [15]. It was additionally found that the kinetics of POA involving both uniaxial and biaxial structures can be theoretically described by using the phenomenological approach suggested in Ref. [18].

In this work, we concentrate on the features of the 3D orientation determined by the above discussed mechanisms of the photoinduced ordering. The different regimes of POA are realized experimentally by choosing appropriate polymers and irradiation conditions. There are two azopolymers of different structure used in this study and the optical anisotropy was induced by irradiating the samples at two different wavelengths. We find that the regime of POA in one of the polymers strongly depends on the wavelength of the exciting light, whereas the other presents the case in which POA is governed by the photoreorientation mechanism regardless of the wavelength.

We show that the experimental results can be interpreted on the basis of the phenomenological model describing the kinetics of POA in terms of angular redistribution probabilities and order parameter correlation functions. This model can be deduced by using the procedure of Refs. [18,31] and is found to give the results that are in good agreement with the experimental data. We also apply the model to calculate the out-of-plane absorbance that cannot be directly estimated from the results of measurements in the regime of photoselection.

The paper is organized as follows. Section II contains the details on the combination of null ellipsometry and absorption methods used in this study as an experimental procedure. The experimentally measured dependencies of birefringence and absorption dichroism on the illumination doses are presented in Sec. III. We draw together these results to unambiguously identify the anisotropy of the orientational structures induced in azopolymer films and to measure the ordering of azochromophores through the absorption order parameter. Anisotropy of the initial structures and of the structures in the regime of photosaturation is found to be uniaxial in both azopolymers. At the early stages of irradiation, the transient anisotropic structures are biaxial. It is shown that under certain conditions, the regime of the kinetics of POA can be changed with the wavelength of the pumping light. We also discuss thermal stability of the photoinduced anisotropy and experimental estimates of the photochemical parameters needed for theoretical calculations. In Sec. IV, we describe the theoretical model formulated by using the phenomenological approach of Refs. [18,31]. We discuss the physical assumptions underlying the model and make brief comments on the derivation of the kinetic equations for the concentrations of isomers and the

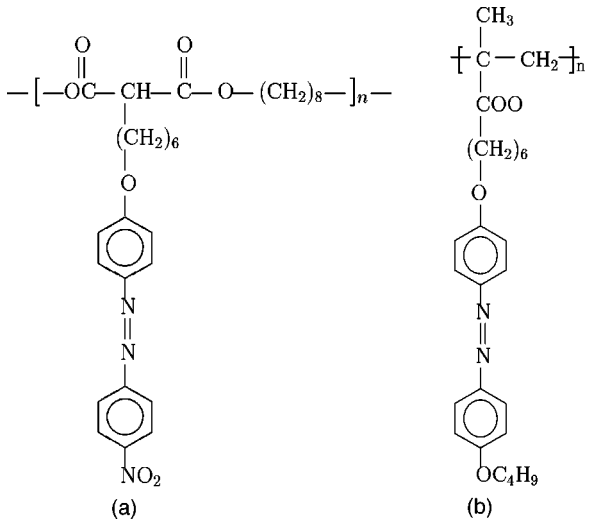

FIG. 1. Chemical structure of polymers. (a) Polymer $P1$, (b) polymer $P2$.

order parameter tensor. In Sec. V, we present numerical results for the absorption coefficients and the order parameters in relation to the irradiation dose calculated by solving the equations of the model. We compare these results with the experimental data and comment on the predictions of the model concerning biaxiality effects, stability, and the regimes of POA. Finally, general discussion of our results and some concluding remarks are given in Sec. VI.

II. EXPERIMENTAL PROCEDURE

A. Polymers

The chemical formulas of two azopolymers used in our experiments are presented in Fig. 1. The details on the synthesis of polymers $P1$ and $P2$ can be found in Ref. [32] and in Ref. [33], correspondingly. The polymers were characterized by elemental analysis and 1H nuclear magnetic resonance spectroscopy. Molecular weight of the polymers was determined by gel permeation chromatography. The average molecular weights of $P1$ and $P2$ are estimated at 13 500 g/mol and 36 000 g/mol, respectively. Both materials are comblike polymers with azobenzene fragments in side chains connected by flexible alkyl spacers to the polymer backbone. The azobenzene chromophore of polymer $P1$ contains polar NO_2 end group that has strong acceptor properties. The azobenzene chromophore of polymer $P2$ contains hydrophobic alkyl tail OC_4H_9. The phase transitions in the polymers were investigated by differential scanning calorimetry and polarization microscopy. Both azopolymers are found to possess liquid crystalline properties in the respective temperature regions. Polymer $P1$ forms smectic A and nematic mesophases within the temperature ranges 44 °C–52 °C and 52 °C–55 °C, respectively. Polymer $P2$ has a nematic mesophase within the temperature interval 112 °C–140 °C. Both polymers are solids at room temperature.

B. Sample preparation

The polymers were dissolved in dichloretane up to concentration 3 wt % and spin coated on the quartz slides. The obtained films were kept at room temperature over 1 day for evaporation of the solvent. The thickness of the films, d, of about 200–600 nm was measured with a profilometer. The uv-visible spectra of the films measured by silicon array spectrometer (OceanOptics Inc.) are presented in Fig. 2. It can be seen that the position of the most intensive absorption band ($\pi\pi^*$ band of azobenzene chromophore) depends on the end substitute of the chromophore. The wavelength of the maximal absorption, λ_{max}, for polymer $P1$ containing chromophore with push-pull properties is shifted to the red as compared to λ_{max} for $P2$.

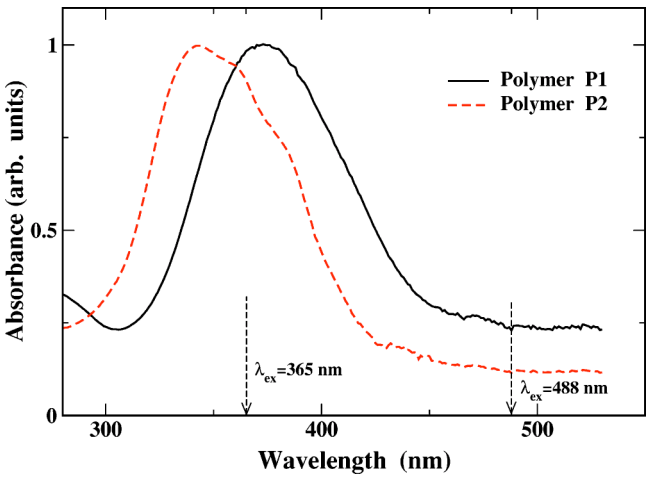

FIG. 2. uv-visible absorption spectra of polymer films.

The anisotropy in the films was induced under irradiation from two different sources of light with different wavelengths λ_{ex} and intensities I:

(1) An Ar^+ laser with $\lambda_{ex}=488$ nm and $I=0.7$ W/cm^2.

(2) A mercury lamp with $\lambda_{ex}=365$ nm and $I=1.5$ mW/cm^2. In this case, the light was selected by an interference filter and polarized with a Glan-Thompson polarization prism.

The wavelengths 365 nm and 488 nm fall into $\pi\pi^*$ and $n\pi^*$ absorption bands of azopolymers, respectively. In both cases, the films were irradiated at normal incidence of the actinic light. The irradiation was carried out in several steps followed by studies of the orientational structure. The resulting time of irradiation was calculated by adding irradiation times of all irradiation steps assuming accumulation of the structural changes. The time interval between irradiation and structural studies was about 15 min. The reason for time delay between these processes will be discussed below.

C. Null ellipsometry method

Instead of the prism coupling methods commonly used for the estimation of principal refractive indices, we applied null ellipsometry technique [34] dealing with birefringence components. By this means we have avoided some disadvantages of the prism coupling method such as the problem of making optical contact between the prism and the polymer layer.

The optical scheme of our method is presented in Fig. 3. The polymer film is placed between crossed polarizer and analyzer and a quarter wave plate with the optic axes ori-

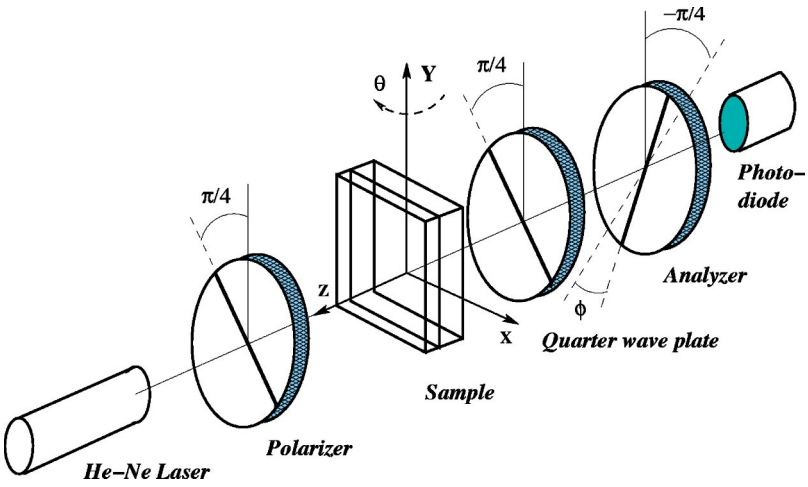

FIG. 3. Null ellipsometry setup.

ented parallel to the polarization direction of the polarizer. The light beam, whose wavelength is far away from the absorption band of the polymer, is passing through the optical system. The elliptically polarized beam passing through the sample is transformed into the linearly polarized light by means of the quarter wave plate. The polarization plane of this light is turned with respect to the polarization direction of the polarizer. This rotation is related to the phase retardation acquired by the light beam after passing through the film under investigation. It can be compensated by rotating the analyzer by the angle ϕ that encodes information on the phase retardation and the in-plane retardation $(n_y-n_x)d$ is $\lambda\,\phi/180$, where n_x, n_y, n_z are the principal refractive indices of the film and λ is the wavelength of light.

This method used for the normal incidence of the testing light is known as the Senarmont technique. It is suitable for the in-plane birefringence measurements.

Using oblique incidence of the testing beam, we have extended this method for estimation of both in-plane n_y-n_x and out-of-plane n_z-n_x birefringences. In this case, the angle ϕ depends on the in-plane retardation $(n_y-n_x)d$, the out-of-plane retardation $(n_z-n_x)d$, and the absolute value of a refractive index of the biaxial film, say, n_x.

We need to have the light coming out of the quarter wave plate almost linearly polarized when the system analyzes the phase shift between two orthogonal eigenmodes of the sample. In our experimental setup, this requirement can be met, when the x axis, directed along the polarization vector of the actinic light, is oriented horizontally or vertically. Dependencies of the analyzer rotation angle ϕ on the incidence angle of the testing beam θ were measured for both vertical and horizontal orientations of the x axis. The value of n_x was measured with the Abbe refractometer independently.

By using Berreman's 4×4 matrix method [35], the θ dependencies of ϕ were calculated. Maxwell's equations for the light propagation through the system of polarizer, sample, and quarter wave plate were solved numerically for the different configurations of optical axes in the samples. The measured and computed ϕ versus θ curves were fitted in the most probable configuration model using the measured value of n_x.

We conclude on the alignment of the azobenzene fragments from the obtained values of $(n_y-n_x)d$ and $(n_z-n_x)d$, assuming that the preferred direction of these fragments coincides with the direction of the largest refractive index. More details on the method can be found in our previous publication [10].

In our setup designed for the null ellipsometry measurements, we used a low power He-Ne laser ($\lambda=632.8$ nm), two Glan-Thompson polarizers mounted on rotational stages from Oriel Corp., a quarter wave plate from Edmund Scientific, and a sample holder mounted on the rotational stage. The light intensity was measured with a photodiode. The setup was automatically controlled by a personal computer. The rotation accuracy of the analyzer was better than 0.2°.

D. Absorption method

The uv-visible absorption measurements were carried out using a diode array spectrometer (OceanOptics). The samples were set normally to the testing beam of a deuterium lamp. A Glan-Thompson prism mounted on a computer-driven stepper was used to control the polarization of the testing beam, $\mathbf{E}_t$.

The uv spectra of both original and irradiated films were measured in the spectral range from 250 nm to 600 nm for the probing light linearly polarized along the x and y axes. From these data, the optical density components D_x and D_y were estimated at the absorption maximum of azochromophores, $\lambda_t=375$ nm (for polymer $P1$) and $\lambda_t=343$ nm (for polymer $P2$).

In general, it is difficult to estimate the out-of-plane absorption coefficient D_z. This, however, can be done in the regime of POA where the fraction of *cis* isomers is negligible (the photoreorientation mechanism) by using the method proposed in Refs. [8,36]. The key point is that the sum of all the principal absorption coefficients, $D_{tot}=D_x+D_y+D_z$, does not depend on irradiation doses. So, if the anisotropy is known to be uniaxial at time t_0 with either $D_x(t_0)=D_z(t_0)$ or $D_y(t_0)=D_z(t_0)$, this will yield the relation

$$D_{tot}=D_x+D_y+D_z=\begin{cases} D_y(t_0)+2D_x(t_0), & \mathbf{n}_o\|\hat{\mathbf{e}}_y, \\ D_x(t_0)+2D_y(t_0), & \mathbf{n}_o\|\hat{\mathbf{e}}_x, \end{cases} \quad (1)$$

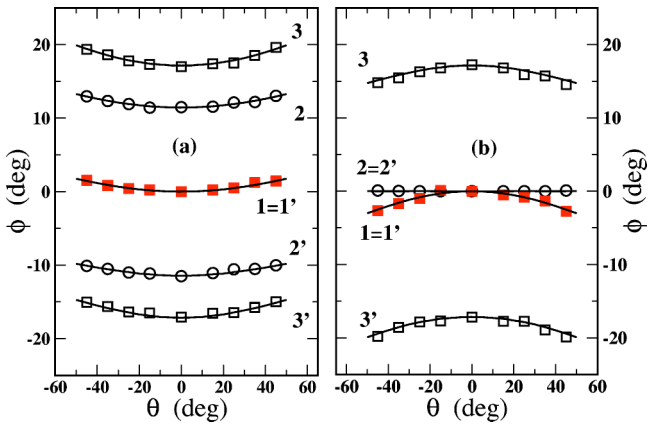

FIG. 4. Measured (circles and squares) and modeled (solid lines) curves for the analyzer angle ϕ vs the incidence angle θ for polymer $P1$ (a) and polymer $P2$ (b). Three cases are shown: (a) nonirradiated films (curves 1 and 1′); (b) photosaturated films at $\lambda_{ex}=365$ nm and $I=1.5$ mW/cm^2 (curves 2 and 2′); and (c) photosaturated films at $\lambda_{ex}=488$ nm and $I=0.7$ W/cm^2 (curves 3 and 3′). The data labeled 1, 2, 3 and 1′, 2′, 3′ are for the x axis of the films in the vertical and horizontal positions, respectively.

where $\mathbf{n}_o$ is the optical axis and $\hat{\mathbf{e}}_i$ is the ith coordinate unit vector. The out-of-plane component D_z can now be computed from Eq. (1). In addition, we calculate the absorption order parameters $S_i^{(a)}$ defined by the expression

$$S_i^{(a)}=\frac{2D_i-D_j-D_k}{2(D_x+D_y+D_z)}, \quad i\neq j\neq k. \tag{2}$$

In Sec. V, we find that in the regime of photoreorientation, the parameters $S_i^{(a)}$ are proportional to the diagonal components of the order parameter tensor of *trans* azochromophores.

III. EXPERIMENTAL RESULTS

A. Nonirradiated films

Figure 4(a) shows the experimentally measured curves of the analyzer angle ϕ versus the incidence angle θ for polymer $P1$. The curve 1 corresponds to the nonirradiated film. The curves measured for the vertical and horizontal positions of the x axis overlap. This implies that the in-plane principal indices n_x and n_y are matched. The film, however, possesses the out-of-plane birefringence. The fitting gives the value $(n_z-n_x)d=-20$ nm. Using the value of the film thickness $d=200$ nm, we have $n_z-n_x=-0.1$ and the relation $n_x=n_y<n_z$ that suggests preferred in-plane alignment with random orientation of azobenzene fragments in the plane of the film. Optically, this structure corresponds to the negative C plate depicted in Fig. 5(a).

Figure 4(b) shows the measured ϕ versus θ curves for polymer $P2$. The results obtained for the nonirradiated film (curve 1) imply that, similar to polymer $P1$, the in-plane birefringence is negligibly small, $\Delta n_{yx}=n_y-n_x\approx 0$. But the film is now characterized by a positive out-of-plane birefringence: $(n_z-n_x)d=35$ nm $(\Delta n_{zx}=n_z-n_x\approx 0.09)$ and $n_z>n_x=n_y$. So, the film of polymer $P2$ is a positive uniaxial medium with the optical axis normal to the film surface [positive C film shown in Fig. 5(b)] and the azobenzene fragments oriented homeotropically.

B. Irradiation at $\lambda_{ex}=365$ nm

1. Polymer P1

The curves 2 and 2′ in Fig. 4(a) show the measured ϕ versus θ curves for polymer $P1$ after 60 min of uv light irradiation. Curves 2 and 2′ correspond to the vertical and horizontal positions of the x axis of the film. Since negative and positive phase shifts at $\theta=0$ correspond to the x axis in the horizontal and vertical directions, respectively, the higher in-plane refractive index is n_y (i.e., in the direction perpendicular to uv light polarization) and the lower one is n_x. Curve fitting gives the following relation between the refractive indices: $n_y-n_x=0.2$ $[(n_y-n_x)d\approx 40$ nm$]$, $(n_z-n_x)d=0$ nm, $n_y>n_x=n_z$. So, the photomodified film is optically equivalent to the positive A plate having optical axis in the plane of the film [Fig. 5(c)]. In this case, the azobenzene fragments show planar alignment perpendicular to the uv light polarization.

The fitted values of the in-plane, $(n_y-n_x)d$, and out-of plane, $(n_z-n_x)d$, retardation for $P1$ corresponding to various irradiation times τ_{ex} are presented in Fig. 6(a). The in-plane birefringence increases and saturates as the irradiation time increases, whereas the out-of-plane birefringence is a decreasing function of the irradiation time and the difference between n_z and n_x becomes negligible in the saturation state. At the early stages of irradiation, all the refractive indices are different, $n_z<n_x<n_y$, and the film is biaxial. In the saturation state, the relation $n_y>n_x=n_z$ implies that the ordering of azobenzene chromophores is uniaxial.

Figure 6(b) represents the results of the absorption measurements for $P1$ film before irradiation and after subsequent irradiation steps. In accord with the null ellipsometry results, after irradiation D_y is above D_x and the azochromophores are aligned along the y direction that is perpendicular to **E**.

The curves $D_x(\tau_{ex})$ and $D_y(\tau_{ex})$ are typical of the photoreorientation mechanism [12,13]. In this case, the fraction of *cis* isomers is negligible and the out-of-plane absorption coefficient D_z depicted in Fig. 6(b) can be estimated by using Eq. (1) to calculate D_{tot} in the photosaturated state where $D_x^{(st)}=D_z^{(st)}$. Figure 6(c) shows the absorption order parameters $S_i^{(a)}$ computed from expression (2).

2. Polymer P2

The curve 2 in Fig. 4(b) shows the measured ϕ versus θ function for the film of $P2$ irradiated with uv light over 60 min. The curves corresponding to the vertical and horizontal positions of the x axis of the film overlap. The fitting gives $n_x=n_y=n_z$ and, thus, the angular distribution of azobenzene chromophores is isotropic.

Figure 7(a) shows the fitted values of $(n_y-n_x)d$ and $(n_z-n_x)d$, obtained for various irradiation times of $P2$. The dependencies of $(n_y-n_x)d$ and $(n_z-n_x)d$ on the irradiation time go through the maximum and saturate at large irradia-

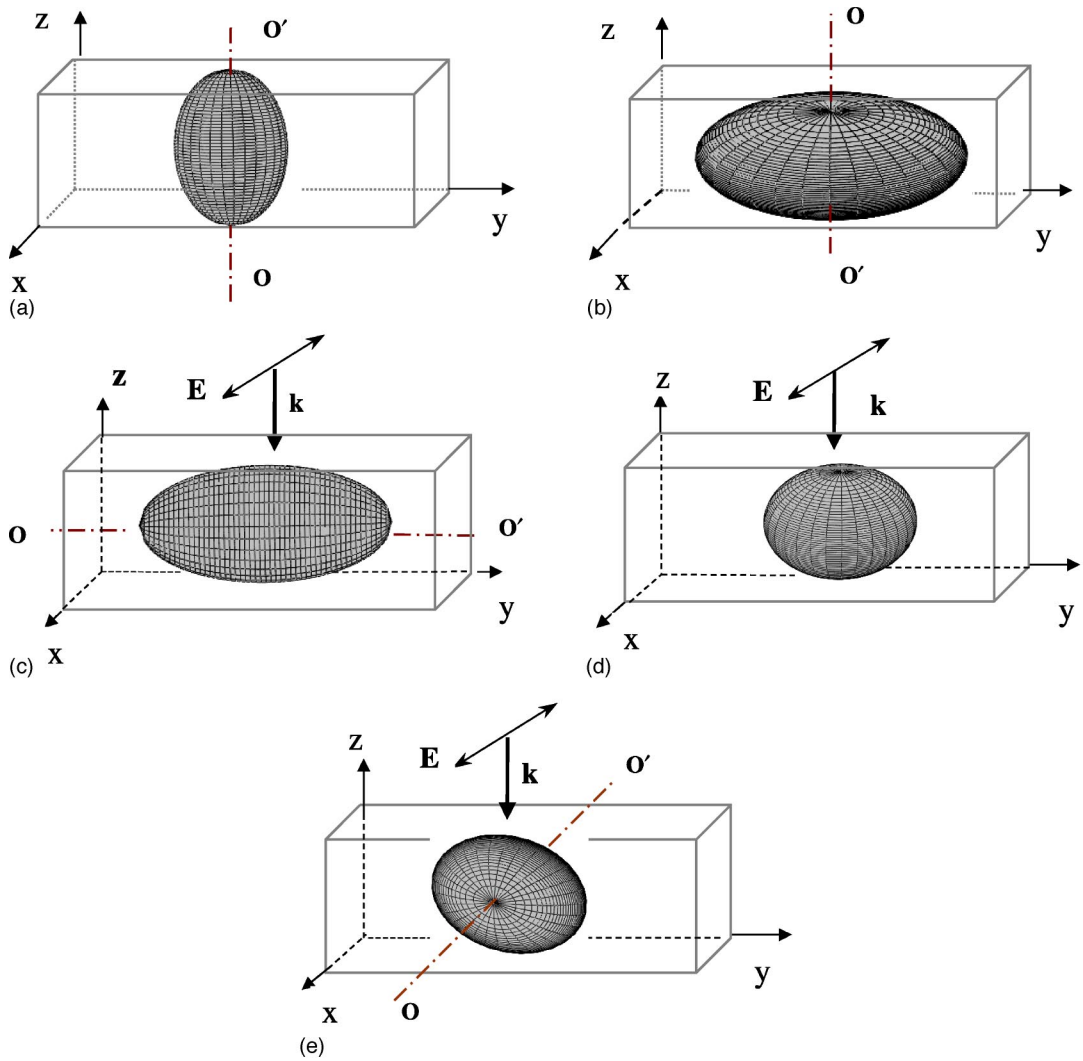

FIG. 5. Ellipsoids of refractive indices for nonirradiated and photosaturated polymer films. (a) Nonirradiated $P2$ polymer with $n_z > n_y = n_x$; (b) nonirradiated $P1$ polymer with $n_z < n_y = n_x$; (c) photosaturated $P1$ polymer with $n_y > n_x = n_z$; (d) photosaturated $P2$ polymer at $\lambda_{ex} = 365$ nm with $n_z = n_y = n_x$; (e) photosaturated $P2$ polymer at $\lambda_{ex} = 488$ nm with $n_x < n_y = n_z$.

tion doses. At the initial irradiation stage $n_z > n_y > n_x$ and the film is biaxial. In the photosaturated state, $n_x = n_y = n_z$ and, as is illustrated in Fig. 5(d), the film is isotropic.

The experimentally measured $D_x(\tau_{ex})$ and $D_y(\tau_{ex})$ curves are shown in Fig. 7(b). Both curves decrease with increasing irradiation dose. This behavior is typical of the mechanism of photoselection [12,13]. In this regime, the exciting light will cause angular selective depopulating of the *trans* state, so that the fraction of *trans* isomers rapidly becomes smaller with illumination time. This process—the so-called angular selective burning—dominates the kinetics of POA and gives rise to diminution of both absorption coefficients D_x and D_y. The isotropy of the photosaturated state then can be explained by negligibly small concentrations of *trans* chromophores at large irradiation doses. This point will be discussed at greater length in Sec. VI.

C. Irradiation at $\lambda_{ex} = 488$ nm

1. Polymer P1

In Fig. 4(a), the curves corresponding to irradiation with $\lambda_{ex} = 488$ nm ($\tau_{ex} = 300$ min) are denoted as 3 and 3′. Similar to the case where $\lambda_{ex} = 365$ nm, the relation between the principal refractive indices is $n_y > n_x = n_z$. So, the induced orientational configurations do not differ and correspond to a uniaxial in-plane alignment with the optical properties of a positive A plate. On the other hand, the value of the in-plane retardation $(n_y - n_x)d$ is considerably higher than it is for $\lambda_{ex} = 365$ nm and reaches 60.

The $(n_y - n_x)d$ and $(n_y - n_x)d$ versus τ_{ex} kinetic curves for the film and irradiation conditions under consideration are presented in Fig. 8(a). The results are qualitatively similar to those obtained for $\lambda_{ex} = 365$ nm: biaxial alignment of the azobenzene chromophores at the early stages of irradia-

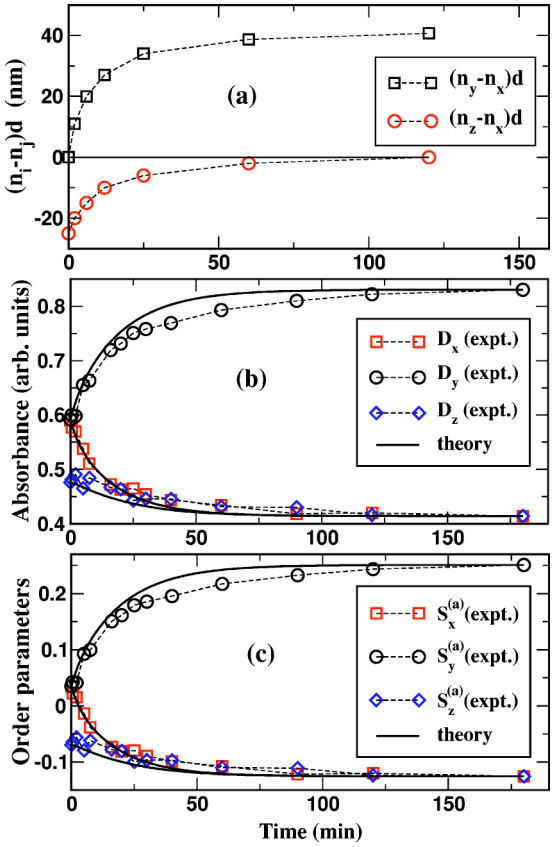

FIG. 6. (a) Birefringence, (b) principal absorption coefficients, and (c) order parameter components as a function of irradiation time at $\lambda_{ex}=365$ nm and $I=1.5$ mW/cm^2 for polymer $P1$.

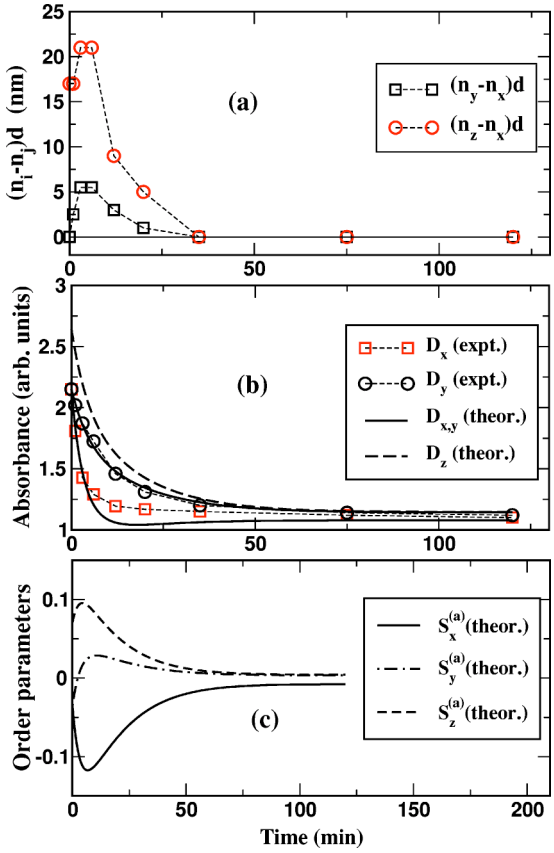

FIG. 7. (a) Birefringence, (b) principal absorption coefficients, and (c) order parameter components as a function of irradiation time at $\lambda_{ex}=365$ nm and $I=1.5$ mW/cm^2 for polymer $P2$.

tion and the uniaxial structure in the photosaturated state. The $D_x(\tau_{ex})$ and $D_y(\tau_{ex})$ curves presented in Fig. 8(b) indicate in-plane angular redistribution of the azobenzene chromophores and the preferential alignment along the direction perpendicular to **E**. In addition, we used Eq. (1) to compute the curve for the out-of-plane component $D_z(\tau_{ex})$ plotted in Fig. 8(b). Figure 8(b) shows dependencies of the absorption order parameters on the irradiation time calculated from Eq. (2).

2. Polymer P2

The curves 3 and 3′ in Fig. 4(b) show the measured ϕ versus θ dependencies for the film of $P2$ irradiated with the actinic light at $\lambda_{ex}=488$ nm over 300 min. As above, the curves corresponding to the vertical and the horizontal position of the x axis are labeled 3 and 3′, respectively. The fitting yields $(n_y-n_x)d=(n_z-n_x)d=60$ nm and $n_y=n_z>n_x$. So, the induced orientational structure is uniaxial. The optical axis of this structure lies in the film plane and is directed along the polarization vector of the actinic light. The principal refractive index for the optical axis direction has the lowest value. The same optical properties possess crystal plate called as negative A plate [Fig. 5(e)]. The negative A plate in the case of azopolymer film stands for random orientation of azochromophores in the plane perpendicular to vector **E**. This is precisely the structure which can be expected from the naive symmetry considerations discussed in Sec. I.

The fitting results $(n_y-n_x)d$ and $(n_y-n_x)d$ plotted as functions of irradiation time τ_{ex} are presented in Fig. 9(a). The curves converge approaching the saturated state. The transient photoinduced structures are biaxial.

The $D_x(\tau_{ex})$ and $D_y(\tau_{ex})$ curves for the case under investigation are shown in Fig. 9(b). In contrast to the case presented in Fig. 7(b), these curves clearly indicate that the regime of POA is dominated by the photoreorientation mechanism [12,13]. So, the out-of-plane coefficient D_z can be estimated by applying the procedure described in Sec. II D to the case in which the known uniaxial structure is represented by the state of saturation with $D_y^{(st)}=D_z^{(st)}$. The curve $D_z(\tau_{ex})$ computed from Eq. (1) and dependencies of the absorption order parameters on the irradiation time are depicted in Figs. 9(b) and 9(c), respectively.

D. The two-step irradiation at $\lambda_{ex}=365$ nm and $\lambda_{ex}=488$ nm

In these experiments, the polymer films were initially irradiated with nonpolarized uv light ($\lambda_{ex}=365$ nm, $I=15$ mW/cm^2) for about 1 h and, subsequently, with the polarized light from Ar^+ laser ($I=0.7$ W/cm^2). The first step of irradiation does not produce considerable changes in the initial structure of polymer $P1$. The $(n_y-n_x)d$ and $(n_y$

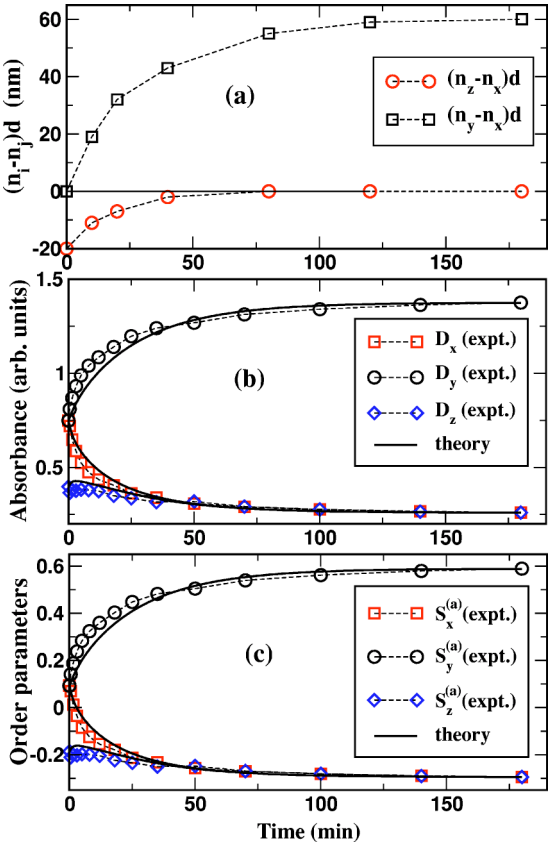

FIG. 8. (a) Birefringence, (b) principal absorption coefficients, and (c) order parameter components as a function of irradiation time at $\lambda_{ex}=488$ nm and $I=0.7$ W/cm^2 for polymer $P1$.

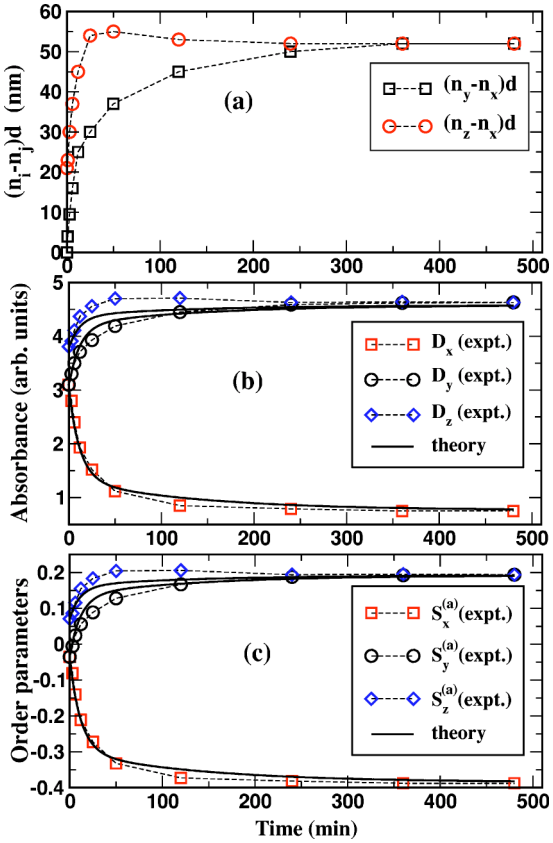

FIG. 9. (a) Birefringence, (b) principal absorption coefficients, and (c) order parameter components as a function of irradiation time at $\lambda_{ex}=488$ nm and $I=0.7$ W/cm^2 for polymer $P2$.

$-n_x)d$ versus τ_{ex} kinetic curves obtained for the second step of irradiation are very close to those obtained for irradiation with only $\lambda_{ex}=488$ nm [see Fig. 8(a)].

After the first step of uv irradiation, $P2$ film was optically isotropic. But similar to the case of the one-step irradiation at $\lambda_{ex}=488$ nm, the subsequent irradiations have generated the anisotropy of a negative A film. The corresponding $(n_y-n_x)d$ and $(n_y-n_x)d$ versus τ_{ex} kinetic curves are presented in Fig. 10. It is seen that preirradiation with uv light strongly accelerates formation of the saturated structure as compared to the case of the one-step irradiation [see Fig. 9(a)]. But for both $P1$ and $P2$ films, this structure in itself is not affected by preirradiation. Thus, the structure is completely determined by the last step of irradiation.

E. Thermal stability of the photoinduced structures

At room temperature, we have not detected any changes in the ordering of nonirradiated films for several weeks. The photoinduced uniaxial and biaxial anisotropies, formed in polymer films after switching off the exciting light, persisted over the same period of time.

We have also studied the influence of the elevated temperatures on the orientational structures. The baking of the nonirradiated $P1$ films at temperatures of mesophases and isotropic phase did not change considerably the initial order. In contrast, $P2$ films had the out-of-plane alignment of azobenzene chromophores enhanced after the treatment at temperatures of both nematic mesophase and isotropic phase. For instance, baking of $P2$ film at 150 °C over 5 min led to the increase in birefringence from $(n_e-n_o)d=35$ nm to $(n_e-n_o)d=55$ nm.

The curing of $P1$ films at the temperatures of nematic and smectic mesophases followed by cooling down to room tem-

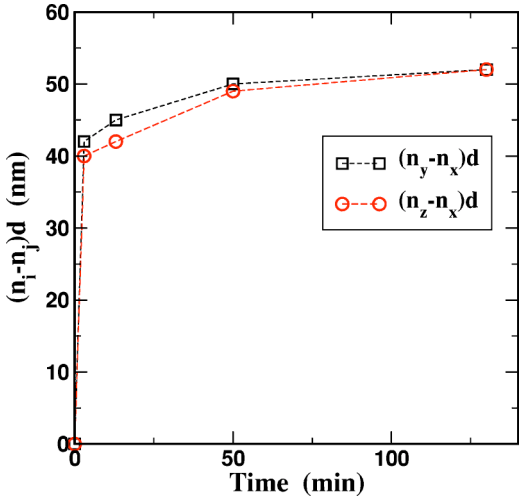

FIG. 10. Birefringence vs irradiation time for the preirradiated polymer $P2$ (see discussion in Sec. III D).

perature destroys biaxiality of the photoinduced structures and enhances the uniaxial anisotropy. Similar effects were observed at the short time (about 5 min) curing in the isotropic state at 70 °C. In this case, the prolonged curing caused the disappearance of the induced anisotropy.

The curing of $P2$ films at temperatures of nematic and isotropic phases transformed the structure of negative uniaxial medium into the positive uniaxial configuration with the azochromophores aligned perpendicular to the film substrate.

F. Photochemical parameters

There are a number of parameters used in subsequent calculations for theoretical interpretation of the experimental results. In this section, we dwell briefly on the experimental results used to estimate the lifetime of the *cis* form, τ_{cis}, and the absorption cross sections of isomers, $\sigma^{(cis)}$ and $\sigma^{(trans)}$.

1. The lifetime of cis isomers

The lifetime τ_{cis} of *cis* isomers was estimated by studying the relaxation of uv spectrum modified by irradiation with nonpolarized light at $\lambda_{ex}=365$ nm. The pumping and testing lights were directed almost normally to the film. The wavelength of the nonpolarized testing light was adjusted at the maximum of $\pi\pi^*$ absorption band of the studied polymer (375 nm and 343 nm for polymers $P1$ and $P2$, respectively).

Temporal evolution of the absorbance after switching off the pumping was measured. The curves then were fitted by using the two-exponential approximation taken in the following form:

$$y(t)=y_0+A_1e^{-t/\tau_1}+A_2e^{-t/\tau_2}. \tag{3}$$

For polymer $P1$, we have $\tau_1=1.2$ s and $\tau_2=1.3$ min with $A_1/A_2\approx 5.3$. The relaxation curve obtained for polymer $P2$ is fitted well by Eq. (3) at $\tau_1=2.6$ min, $\tau_2=440$ min, and $A_1/A_2\approx 0.13$.

In the case of polymer $P1$, relaxation is dominated by the fast component that corresponds to the largest amplitude and can be attributed to *cis-trans* backward isomerization of the chromophores trapped in a strained conformation [37]. The lifetime can now be estimated as a decay time for the bulk of *cis* isomers to yield $\tau_{cis}\approx 1.2$ s.

The origin of slower and less pronounced component could be caused by thermal *cis-trans* isomerization of the other fraction of azobenzene moieties, which are strongly restricted in their molecular dynamics by the polymer matrix. Their reaction requires a stronger reorganization of the polymer film [38]. Since the waiting time in our experiments was about 15 min, we can safely assume all *cis* isomers in polymer $P1$ relaxed back to the *trans* isomeric form.

For polymer $P2$, the largest contribution comes from the slowest component with $\tau_2=440$ min. This time gives an estimate for the lifetime of *cis* isomers, $\tau_{cis}\approx 440$ min.

There is a difficulty in estimating τ_{cis} with this method. In addition to *trans-cis* photoisomerization, the uv spectrum can also be influenced by photoreorientation. The nonpolarized light may cause the out-of-plane reorientation of azobenzene chromophores reducing the uv absorption. This out-of-plane reorientation, however, cannot be effective in polymer $P1$, which shows strong preference to in-plane reorientation. For polymer $P2$, the out-of-plane reorientation of azochromophores has been additionally checked by the absorption measurement at the oblique incidence of testing beam. An increase in the polymer absorption at 343 nm under uv irradiation has not been detected. Thus it is safe to assume that the observed relaxation can be solely attributed to *cis-trans* thermal isomerization.

2. Absorption cross sections

The above mentioned photoinduced reorientation accompanying photochemical process makes it extremely difficult to estimate the coefficients of the molecular extinction in polymer films. For this purpose, we applied the method well known for polymer solutions [39]. Both polymers were dissolved in toluene at concentration 5×10^{-3} g/l. The uv-visible spectra of the polymer solutions were measured before and during irradiation. In the latter case, the solutions were in the photosaturated state. Each spectrum was decomposed into three components of the Gaussian shape denoted as $D_c^{(i)}(\lambda)$, $D_t^{(i)}(\lambda)$, and $D_n^{(i)}(\lambda)$ in the expression

$$D^{(i)}(\lambda)=D_c^{(i)}(\lambda)+D_t^{(i)}(\lambda)+D_n^{(i)}(\lambda), \tag{4}$$

where the index i labels the spectra of the nonirradiated ($i=0$) and the irradiated solution ($i=1$). The first two terms on the right-hand side of Eq. (4), $D_c^{(i)}(\lambda)$ and $D_t^{(i)}(\lambda)$, can be assigned to $\pi\pi^*$ absorption of *cis* and *trans* isomers, respectively. The last term $D_n^{(i)}(\lambda)$ corresponds to $n\pi^*$ absorption where the contributions from *cis* and *trans* isomers cannot be separated.

We can now relate the components $D_t^{(i)}$ and $D_c^{(i)}$ to the $\pi\pi^*$ absorption cross sections of isomers, $\sigma_\pi^{(cis)}$ and $\sigma_\pi^{(trans)}$, and the concentrations of isomers, $C_{trans}^{(i)}$ and $C_{cis}^{(i)}$, in the nonirradiated film ($i=0$) and in the photosaturated ($i=1$) state as follows:

$$D_t^{(i)}(\lambda)=dC_{trans}^{(i)}\sigma_\pi^{(trans)}(\lambda), \tag{5a}$$

$$D_c^{(i)}(\lambda)=dC_{cis}^{(i)}\sigma_\pi^{(cis)}(\lambda), \tag{5b}$$

$$C=C_{trans}^{(i)}+C_{cis}^{(i)}, \quad i=0,1, \tag{5c}$$

where d is the cell thickness, C is the experimentally measured total concentration of the dissolved molecules. Solving system (5) yields the cross sections $\sigma_\pi^{(\alpha)}$ and the concentrations $C_\alpha^{(i)}$ ($\alpha=trans,cis$) which can be further employed to determine the absorption cross sections $\sigma_n^{(\alpha)}$ in the overlapping $n\pi^*$ absorption bands of isomers from the relation

$$D_n^{(i)}=(\sigma_n^{(trans)}C_{trans}^{(i)}+\sigma_n^{(cis)}C_{cis}^{(i)})d. \tag{6}$$

The average absorption cross section of *trans* isomers $\sigma^{(trans)}$ and the cross section of *cis* isomers $\sigma^{(cis)}$ at the wavelength λ can now be computed as a sum of $\sigma_\pi^{(\alpha)}(\lambda)$ and $\sigma_n^{(\alpha)}(\lambda)$. The resulting estimates for the absorption cross sec-

TABLE I. Photochemical parameters. The last entry gives the parameter r from Eq. (22) with γ_{cis}, q_{cis}, and q_{trans} defined in Eqs. (11) and (13). This parameter determines the regime of POA (see discussion in Sec. V).

Polymer $P1$			Polymer $P2$		
λ_{ex} (nm)	365	488	λ_{ex} (nm)	365	488
I (mW/cm^2)	1.5	700	I (mW/cm^2)	1.5	700
$\sigma^{(cis)}$ (10^{-19} cm^2)	24.8	0.8	$\sigma^{(cis)}$ (10^{-19} cm^2)	6.0	1.1
$\sigma^{(trans)}/\sigma^{(cis)}$	5.6	0.47	$\sigma^{(trans)}/\sigma^{(cis)}$	57.0	0.2
$\sigma_{\parallel}^{(trans)}/\sigma_{\perp}^{(trans)}$	6.95	36.2	$\sigma_{\parallel}^{(trans)}/\sigma_{\perp}^{(trans)}$	9.4	39.6
$\Phi_{cis\to trans}$ (%)	10	10	$\Phi_{cis\to trans}$ (%)	5	10
$\Phi_{trans\to cis}$ (%)	10	10	$\Phi_{trans\to cis}$ (%)	10	10
$(\gamma_{cis}+q_{cis}I)/(q_{trans}I)$	623.4	2181	$(\gamma_{cis}+q_{cis}I)/(q_{trans}I)$	0.03	69.1

tions of the polymers calculated at the wavelengths of the exciting light are given in Table I.

IV. MODEL

Theoretical considerations of this section deal with the kinetics of POA that determines how the amount of photoinduced anisotropy characterized by either absorption dichroism or birefringence evolves in time upon illumination and after switching it off. Below we briefly discuss the simple phenomenological model describing the kinetics of POA in terms of the order parameter tensor and the concentrations of azochromophores. (More details on the model and the underlying phenomenological approach can be found in Refs. [18,31].)

We shall assume that the azobenzene groups in the ground state are of *trans* form (*trans* molecules) and the orientation of the molecular axis is defined by the unit vector $\hat{\mathbf{n}} = (\sin\theta\cos\phi,\ \sin\theta\sin\phi,\ \cos\theta)$, where θ and ϕ are polar and azimuth angles of the unit vector. Angular distribution of the *trans* molecules at time t is characterized by the number distribution function $N_{trans}(\hat{\mathbf{n}},t)$. Similarly, azochromophores in the excited state have the *cis* conformation (*cis* molecules) and are characterized by the function $N_{cis}(\hat{\mathbf{n}},t)$. Then the number of *trans* and *cis* molecules is given by

$$N_{trans}(t) \equiv N n_{trans}(t) = \int N_{trans}(\hat{\mathbf{n}},t)\, d\hat{\mathbf{n}}, \tag{7}$$

$$N_{cis}(t) \equiv N n_{cis}(t) = \int N_{cis}(\hat{\mathbf{n}},t) d\hat{\mathbf{n}}, \tag{8}$$

where $\int d\hat{\mathbf{n}} \equiv \int_0^{2\pi} d\phi \int_0^{\pi} \sin\theta\, d\theta$ and N is the total number of molecules. The normalized angular distribution functions $f_\alpha(\hat{\mathbf{n}},t)$ of *trans* ($\alpha = trans$) and *cis* ($\alpha = cis$) molecules can be conveniently defined by the relation $N_\alpha(\hat{\mathbf{n}},t) = N n_\alpha(t) f_\alpha(\hat{\mathbf{n}},t)$.

The kinetic rate equations for $N_\alpha(\hat{\mathbf{n}},t)$ are taken in the following form of master equations [18]:

$$\begin{aligned}\frac{\partial N_\alpha}{\partial t} = \int & [W(\alpha,\hat{\mathbf{n}}|\beta,\hat{\mathbf{n}}')N_\beta(\hat{\mathbf{n}}',t) \\ & - W(\beta,\hat{\mathbf{n}}'|\alpha,\hat{\mathbf{n}})N_\alpha(\hat{\mathbf{n}},t)]d\hat{\mathbf{n}}' \\ & + \gamma_\alpha\Big[N_\alpha(t)\int \Gamma_{\alpha\text{-}p}(\hat{\mathbf{n}},\hat{\mathbf{n}}')f_p(\hat{\mathbf{n}}',t)d\hat{\mathbf{n}}' \\ & - N_\alpha(\hat{\mathbf{n}},t)\Big], \quad \alpha \neq \beta, \end{aligned} \tag{9}$$

where $\alpha,\beta \in \{trans,cis\}$ and the angular distribution function $f_p(\hat{\mathbf{n}},t)$ characterizes the anisotropic field due to interaction between a side chain fragment and nearby molecules.

In particular, this field is affected by collective degrees of freedom of nonabsorbing units such as main chains and determines angular distribution of the molecules in the stationary regime. It bears close resemblance to the equilibrium distribution of the mean field theories of POA [22,23,40].

So, we have the additional subsystem characterized by $f_p(\hat{\mathbf{n}},t)$ attributed to the presence of long-living angular correlations coming from anisotropic interactions between azochromophores and collective modes of polymeric environment. For brevity, we shall refer to the subsystem as the polymer system and write down the kinetic equation for the distribution function $f_p(\hat{\mathbf{n}},t)$ in the form

$$\begin{aligned}\frac{\partial f_p(\hat{\mathbf{n}},t)}{\partial t} = - \sum_{\alpha=\{trans,cis\}} & \gamma_p^{(\alpha)} n_\alpha(t)\Big[f_p(\hat{\mathbf{n}},t) \\ & - \int \Gamma_{p\text{-}\alpha}(\hat{\mathbf{n}},\hat{\mathbf{n}}')f_\alpha(\hat{\mathbf{n}}',t)d\hat{\mathbf{n}}'\Big]. \end{aligned} \tag{10}$$

Equations (9) and (10) can be used to formulate a number of phenomenological models of POA and, as is shown in Ref. [31], the results of Refs. [14,22–24,40] can be recovered by choosing suitably defined angular redistribution probabilities $\Gamma_{\beta\text{-}\alpha}(\hat{\mathbf{n}},\hat{\mathbf{n}}')$.

We can now describe the transition rates $W(\alpha,\hat{\mathbf{n}}|\beta,\hat{\mathbf{n}}')$ from Eq. (9). The rate of *trans-cis* photoisomerization stimulated by the incident uv light enters the first bracketed term

on the right-hand side of Eq. (9). For the electromagnetic wave linearly polarized along the x axis, this rate can be written as follows [12,41]:

$$W(cis,\hat{\mathbf{n}}|trans,\hat{\mathbf{n}}')=\Gamma_{trans\text{-}cis}(\hat{\mathbf{n}},\hat{\mathbf{n}}')P_{trans}(\hat{\mathbf{n}}'), \quad (11)$$

$$P_{trans}(\hat{\mathbf{n}})=(\hbar\omega_{trans})^{-1}\Phi_{trans\to cis}\sum_{i,j}\sigma_{ij}^{(trans)}(\hat{\mathbf{n}})E_iE_j^* = q_{trans}I(1+un_x^2), \quad (12)$$

where $\boldsymbol{\sigma}^{(trans)}(\hat{\mathbf{n}})$ is the tensor of absorption cross section for the *trans* molecule oriented along $\hat{\mathbf{n}}$: $\sigma_{ij}^{(trans)}=\sigma_{\perp}^{(trans)}\delta_{ij}+(\sigma_{\parallel}^{(trans)}-\sigma_{\perp}^{(trans)})n_in_j$; $u\equiv(\sigma_{\parallel}^{(trans)}-\sigma_{\perp}^{(trans)})/\sigma_{\perp}^{(trans)}$ is the absorption anisotropy parameter; $\hbar\omega_{trans}$ is the photon energy; $\Phi_{trans\to cis}$ is the quantum yield of the process and $\Gamma_{trans\text{-}cis}(\hat{\mathbf{n}},\hat{\mathbf{n}}')$ describes the angular redistribution of the molecules excited in the *cis* state; I is the pumping intensity and $q_{trans}\equiv(\hbar\omega_{trans})^{-1}\Phi_{trans\to cis}\sigma_{\perp}^{(trans)}$.

Similarly, the rate of *cis-trans* transition is

$$W(trans,\hat{\mathbf{n}}|cis,\hat{\mathbf{n}}')=(\gamma_{cis}+q_{cis}I)\Gamma_{cis\text{-}trans}(\hat{\mathbf{n}},\hat{\mathbf{n}}'), \quad (13)$$

where $q_{cis}\equiv(\hbar\omega_{trans})^{-1}\Phi_{cis\to trans}\sigma^{(cis)}$ and $\gamma_{cis}\equiv 1/\tau_{cis}$, τ_{cis} is the lifetime of *cis* fragments and the anisotropic part of the absorption cross section is disregarded, $\sigma_{\parallel}^{(cis)}=\sigma_{\perp}^{(cis)}\equiv\sigma^{(cis)}$. In the model under consideration, the angular redistribution probabilities $\Gamma_{trans\text{-}cis}$ and $\Gamma_{cis-trans}$ are both assumed to be isotropic and equal to $(4\pi)^{-1}$.

The last square bracketed term on the right-hand side of Eq. (9) describes the process that equilibrates the side chain absorbing molecules and the polymer system in the absence of irradiation. If there is no angular redistribution, then $\Gamma_{\alpha\text{-}p}(\hat{\mathbf{n}},\hat{\mathbf{n}}')=\delta(\hat{\mathbf{n}}-\hat{\mathbf{n}}')$ and both equilibrium angular distributions $f_{trans}^{(eq)}$ and $f_{cis}^{(eq)}$ are equal to f_p.

Since we have neglected the anisotropy of *cis* fragments in Eq. (13), it is reasonable to suppose that the equilibrium distribution of *cis* molecules is also isotropic, $f_{cis}^{(eq)}=f_{iso}\equiv(4\pi)^{-1}$, so that $\gamma_{cis}=\gamma_p^{(cis)}=0$. On the other hand, we assume that there is no angular redistribution and the equilibrium angular distribution of *trans* fragments is determined by the polymer system: $f_{trans}^{(eq)}=f_p$.

Equilibrium properties of *cis* and *trans* isomers are thus characterized by two different equilibrium angular distributions: f_{iso} and f_p, respectively. It means that in our model, the anisotropic field represented by f_p does not influence the angular distribution of nonmesogenic *cis* fragments.

From Eqs. (9), (11), and (13), it is not difficult to deduce the equation for $n_{trans}(t)$:

$$\frac{\partial n_{trans}}{\partial t}=(\gamma_{cis}+q_{cis}I)n_{cis}-\langle P_{trans}\rangle_{trans}n_{trans}, \quad (14)$$

where the angular brackets $\langle\cdots\rangle_{\alpha}$ stand for averaging over angles with the distribution function f_{α}. Remarkably, this equation does not depend on the form of the angular redistribution probabilities.

Similarly, the kinetic equations for the angular distribution functions of isomers f_{α} and of the polymer system f_p can also be derived [31]. It is, however, more suitable to describe the temporal evolution of photoinduced anisotropy in terms of the components of the order parameter tensor [42]

$$S_{ij}(\hat{\mathbf{n}})=2^{-1}(3n_in_j-\delta_{ij}). \quad (15)$$

Integrating the equations for the angular distribution functions multiplied by $S_{ij}(\hat{\mathbf{n}})$ over the angles will provide a set of equations for the averaged order parameter components $S_{ij}^{(\alpha)}\equiv\langle S_{ij}(\hat{\mathbf{n}})\rangle_{\alpha}$.

The result for the order parameters of *cis* molecules is that initially isotropic (and equilibrium) angular distribution of *cis* fragments remains unchanged in the course of irradiation and we have no effects due to the ordering kinetics of *cis* molecules in this model [31].

The procedure described in Ref. [31] can now be used to yield the resulting system of kinetic equations for the diagonal components of the order parameter tensor characterizing *trans* molecules and the polymer system,

$$n_{trans}\frac{\partial S}{\partial t}=-2u/3q_{trans}I(5/7+2\lambda/7S-\lambda^2S^2)n_{trans}-(\gamma_{cis}+q_{cis}I)n_{cis}S+\gamma_{trans}n_{trans}(S_p-S), \quad (16)$$

$$n_{trans}\frac{\partial\Delta S}{\partial t}=2u/3q_{trans}I\lambda(2/7+\lambda S)n_{trans}\Delta S-n_{cis}(\gamma_{cis}+q_{cis}I)\Delta S+\gamma_{trans}n_{trans}(\Delta S_p-\Delta S), \quad (17)$$

$$\frac{\partial S_p}{\partial t}=-\gamma_pn_{trans}(S_p-S), \quad (18)$$

$$\frac{\partial\Delta S_p}{\partial t}=-\gamma_pn_{trans}(\Delta S_p-\Delta S), \quad (19)$$

where $\gamma_p\equiv\gamma_p^{(trans)}$, $S\equiv\langle S_{xx}\rangle_{trans}$, $\Delta S\equiv\langle S_{yy}-S_{zz}\rangle_{trans}$, $S_p\equiv\langle S_{xx}\rangle_p$, and $\Delta S_p\equiv\langle S_{yy}-S_{zz}\rangle_p$.

The key point of the approach suggested in Ref. [31] is the assumption that the order parameter correlation functions (correlators)

$$G_{ij;mn}=\langle S_{ij}(\hat{\mathbf{n}})S_{mn}(\hat{\mathbf{n}})\rangle_{trans}-S_{ij}^{(trans)}S_{mn}^{(trans)}, \quad (20)$$

which characterize response of the side groups to the pumping light and enter the kinetic equations for the order parameter components of *trans* molecules, can be expressed in terms of the averaged order parameters $S_{ij}^{(trans)}$.

It was shown that the parabolic approximation used in Ref. [18] can be improved by rescaling the order parameter components: $\langle S_{ii}\rangle_{trans}\to\lambda\langle S_{ii}\rangle_{trans}$ with $\lambda=(1+0.6\sqrt{30})/7$ computed from the condition that there are no fluctuations provided the molecules are perfectly aligned along the coordinate unit vector $\hat{\mathbf{e}}_i$: $G_{ii;ii}=0$ at $\langle S_{ii}\rangle_{trans}=1$. In Ref. [31], this heuristic procedure has also been found to provide a reasonably accurate approximation for the correlators calcu-

lated by assuming that the angular distribution of mesogenic groups in azopolymers can be taken in the form of distribution functions used in the variational mean field theories of liquid crystals [42,43].

Our last remark in this section concerns polymer $P1$ where the part of the correlation functions responsible for the out-of-plane reorientation appears to be suppressed by polymeric environment. As in Ref. [18], we shall account for the presence of these constraints by assuming that $G_{ij;\,xx} \approx -G_{ij;\,yy}$. The result is that the equations for the diagonal order parameter components will be in the form of Eqs. (16)–(19), where we need to change the sign of the first term on the right hand sides of Eqs. (16) and (17) and to interchange S_{xx} and S_{yy}.

V. NUMERICAL RESULTS

In this section, we employ our model to interpret the experimental data of the uv absorption measurements for different irradiation doses. The principal absorption coefficients D_i can be related to the concentrations and the order parameters as follows:

$$D_i \propto \langle \sigma_{ii}^{(trans)} \rangle_{trans} n_{trans} + \sigma^{(cis)} n_{cis} \propto [1 + u^{(a)}(2S_i + 1)/3] n_{trans} + q_{cis\text{-}trans} n_{cis}, \quad (21)$$

where $S_i \equiv \langle S_{ii} \rangle_{trans}$, $u^{(a)}$ is the absorption anisotropy parameter, and $q_{cis\text{-}trans}$ is the ratio of $\sigma^{(cis)}$ and $\sigma_{\perp}^{(trans)}$ at the wavelength of probing light.

Equation (21) implies that the method of total absorption based on Eq. (1) is applicable when the fraction of *cis* fragments is negligible, $n_{cis} \approx 0$. In this case from Eq. (21), the absorption order parameters (2) are proportional to S_i: $S_i^{(a)} = u^{(a)}/(3 + u^{(a)}) S_i$.

The theoretical curves are computed by solving the kinetic equations of the model discussed in the preceding section. The initial values of the order parameters $S(0)$ and $\Delta S(0)$ are taken from the experimental data measured at $\lambda_{ex} = 488$ nm. Since the system is initially at the equilibrium state, the remaining part of the initial conditions is as follows: $S_p(0) = S(0)$, $\Delta S_p(0) = \Delta S(0)$, $n_{trans}(0) = 1$, and $n_{cis}(0) = 0$.

The anisotropy of nonirradiated films is uniaxial for both polymers: $S_z^{(a)}(0) = -0.18 < S_x^{(a)}(0) = S_y^{(a)}(0) = 0.09$ (polymer $P1$) and $S_z^{(a)}(0) = 0.07 > S_x^{(a)}(0) = S_y^{(a)}(0) = -0.035$ (polymer $P2$). On the other hand, reaching the photosteady state orientational structure of the polymers is characterized by different uniaxial anisotropies: $S_x^{(st)} = S_z^{(st)} < S_y^{(st)}$ (polymer $P1$) and $S_x^{(st)} < S_y^{(st)} = S_z^{(st)}$ (polymer $P2$). So, as is shown in Figs. 6–9, the transient anisotropic structures are inevitably biaxial. These biaxial effects are related to the difference between the initial anisotropy of polymer films and the anisotropy of the photosaturated state.

Numerical calculations in the presence of irradiation were followed by computing the stationary values of S and ΔS to which the order parameters decay after switching off the irradiation at time t_0. For polymer $P2$, the lifetime of the *cis* fragments was found to be much longer than the periods examined and we can safely neglect γ_{cis}. If $\gamma_{cis} = 0$, the kinetic equations in the absence of irradiation can be easily solved to yield the stationary value of S_i and $S_i^{(p)}$: $[\gamma_p n_{trans}(t_0) S_i(t_0) + \gamma_{trans} S_i^{(p)}(t_0)]/\gamma$, where $\gamma \equiv \gamma_p n_{trans}(t_0) + \gamma_{trans}$. There is no further relaxation after reaching this stationary state and its anisotropy is long term stable. The lifetime of *cis* forms in polymer $P1$ is $\tau_{cis} = 1.2$ s and the kinetic equations need to be solved numerically. This, however, does not affect the conclusion about the long term stability of POA.

According to Ref. [14], the relaxation time characterizing the decay of $D_i(t)$ to its stationary value after switching off the irradiation in polymer $P1$ can be estimated at about $\tau_t = 15$ min. The experimental estimate for polymer $P2$ is $\tau_t = 30$ min. The theoretical value of this relaxation time, deduced from the solution of the kinetic equations in the absence of irradiation, is $\tau_{trans} \approx 1/(\gamma_p + \gamma_{trans})$. So, in the simplest case, we can assume both relaxation times, τ_p ($\gamma_p = 1/\tau_p$) and τ_{trans} ($\gamma_{trans} = 1/\tau_{trans}$), to be equal to 30 min ($P1$) and 60 min ($P2$). Table I shows the estimates for the absorption cross section of *cis* molecules $\sigma^{(cis)}$ and the average absorption cross section of *trans* fragments, $\sigma^{(trans)} = (\sigma_{||}^{(trans)} + 2\sigma_{\perp}^{(trans)})/3$, obtained from the uv spectra of the polymers dissolved in toluene.

For these polymers, the absorption anisotropy parameters and the quantum efficiencies are unknown and need to be fitted. We used the value of S_{st} as an adjustable parameter, so that the anisotropy parameters u and $u^{(a)}$ can be derived from Eq. (23) and from the experimental value of the absorption order parameter $S_{st}^{(a)}$ measured at $\lambda_{ex} = 488$ nm in the photosteady state.

The numerical results presented in Figs. 6–9 are computed at $u^{(a)} = 13.0$ and $q_{cis\text{-}trans} = 2.9$ (polymer $P1$); $u^{(a)} = 11.0$ and $q_{cis\text{-}trans} = 2.15$ (polymer $P2$). The quantum efficiencies are listed in Table I and are of the same order of magnitude as the experimental values for other azobenzene compounds [44].

In order to characterize the regime of POA, we can use the fraction of *cis* fragments in the photostationary state. From Eq. (14), this fraction is given by

$$n_{cis}^{(st)} = \frac{3 + u(1 + 2S_{st})}{3(r+1) + u(1 + 2S_{st})}, \quad (22)$$

where $r \equiv (\gamma_{cis} + q_{cis} I)/(q_{trans} I)$, $S_{st} \equiv S_x^{(st)}$, and the corresponding value of the order parameter is a solution of the following equation:

$$2u\,(1/5 + 2\lambda/7\, S_{st} - \lambda^2 S_{st}^2) = -S_{st}[3 + u(1 + 2S_{st})], \quad (23)$$

deduced by using Eqs. (16) and (18).

At small values of r, Eq. (22) will yield the fraction $n_{cis}^{(st)}$ that is close to the unity and we have the kinetics of POA in the regime of photoselection. In the opposite case of sufficiently large values of r, the photosteady fraction of *cis* molecules will be very small that is typical of the photoreorientation mechanism.

When, as in polymer $P1$, *cis* isomers are short living, so that the rate of thermal relaxation γ_{cis} is relatively large, the values of the parameter r listed in Table I are large at both wavelengths of the exciting light. In this case, the fractions of *cis* isomers in the photosaturated state computed from Eqs. (22) and (23) are negligibly small: $n_{cis}^{(st)} \approx 0.003$ at $\lambda_{ex} = 365$ nm and $n_{cis}^{(st)} \approx 0.002$ at $\lambda_{ex} = 488$ nm. So, we have the kinetics of POA in the regime of photoreorientation. It is illustrated in Figs. 6(b) and 8(b), where the measured and the calculated curves are in good agreement and correspond to the photoreorientation mechanism.

In polymer $P2$, *cis* isomers are long living with negligibly small relaxation rate γ_{cis}. The parameter r is now the ratio of the rates $q_{cis}I$ and $q_{trans}I$ that characterize $cis \rightarrow trans$ and $trans \rightarrow cis$ stimulated transitions, correspondingly. This ratio is determined by the quantum efficiencies $\Phi_{trans \rightarrow cis}$ and $\Phi_{cis \rightarrow trans}$, and the absorption cross sections $\sigma_{\perp}^{(trans)}$ and σ_{cis}. In this case, we can have both mechanisms depending on the wavelength of excitation.

Figure 9 presents the case in which the wavelength of light is far from the absorption maximum, $\lambda_{ex} = 488$ nm. It is seen that, similar to polymer $P1$, the kinetics of the absorption coefficients, presented in Fig. 9(b), is typical for the photoreorientation mechanism. According to Table I, the value of r is 69.1 and we can use Eqs. (22) and (23) to estimate the fraction $n_{cis}^{(st)}$ at about 0.02. It means that in this case, the $cis \rightarrow trans$ transitions stimulated by the exciting light will efficiently deplete the *cis* state and the absorption coefficients are controlled by the terms proportional to the order parameter of *trans* molecules [see Eq. (21)].

In contrast, Fig. 7(b) shows that the experimental dependencies for both D_x and D_y are decreasing functions of the irradiation time at the wavelength $\lambda_{ex} = 365$ nm near the maximum of absorption band. It indicates that the kinetics of POA is governed by the mechanism of photoselection. In this case, we have $r = 0.03$ and $n_{cis}^{(st)} = 0.98$. The method described in Sec. II D is now inapplicable, so the out-of-plane absorption coefficient D_z and the order parameters $S_i^{(a)}$ can only be estimated theoretically. These curves calculated from our model are shown in Figs. 7(b) and 7(c).

VI. DISCUSSION AND CONCLUSIONS

In Sec. V, we have introduced the parameter r that can be written as the ratio of the characteristic time of *trans-cis* isomerization, $\tau_{ex} = 1/(q_{trans}I)$, to the time characterizing the decay of the *cis* state in the presence of irradiation, $\tilde{\tau}_{cis} = 1/(\gamma_{cis} + q_{cis}I)$. We have also shown that depending on the value of this parameter, the kinetics of POA is governed by either photoselection or photoreorientation mechanisms.

For large values of r, $r \gg 1$, we have $\tilde{\tau}_{cis} \ll \tau_{ex}$, so that the lifetime of *cis* isomers under irradiation $\tilde{\tau}_{cis}$ is short and the isomers are short living. In this case, the photoreorientation mechanism is found to dominate the kinetics of POA. The opposite case of small values of r characterizes the regime of photoselection, where $\tilde{\tau}_{cis} \gg \tau_{ex}$ and *cis* isomers are long living in the presence of irradiation.

It should be stressed that the mechanism of photoselection cannot occur in polymers with high rate of thermal *cis-trans* isomerization γ_{cis}, where the time of *trans-cis* isomerization τ_{ex} is longer than the lifetime of *cis* isomers $\tau_{cis} = 1/\gamma_c > \tilde{\tau}_{cis}$. In our study, this case is represented by polymer $P1$ in which the mechanism of photoreorientation dominates at both wavelengths of excitation.

In polymer $P2$, γ_{cis} is very small and the relaxation time $\tilde{\tau}_{cis}$ is determined by the rate of *cis-trans* photoisomerization $q_{cis}I$. When the wavelength of the exciting light is in $n\pi^*$ absorption band of azochromophores, this rate is higher than the rate of *trans-cis* isomerization, $q_{trans}I$. So, at $\lambda_{ex} = 488$ nm the photoreorientation mechanism dominates in both polymers.

In contrast to the $n\pi^*$ absorption band, $\pi\pi^*$ absorption bands of isomers are well separated. The wavelength $\lambda_{ex} = 365$ nm lies within $\pi\pi^*$ absorption band of *trans* chromophores, so that the rate $q_{cis}I$ is low as compared to $q_{trans}I$. For polymer $P2$, this means that there is nothing to prevent the *cis* state from being populated under the action of uv light and the kinetics of POA is now governed by the mechanism of photoselection.

The photochemical properties of azopolymers are determined in large part by the molecular structure of azochromophores, which incorporates the azobenzene core and substitutes. For instance, sufficiently polarized azochromophores (push-pull chromophores) usually have short-living *cis* isomers. On the other hand, the chromophores containing long alkyl substitutes are characterized by long-living *cis* form. Our results show that the polymers under consideration comply with these rules.

In addition, the molecular structure of azopolymers determines self-organization of azochromophores, which in turn affects 3D orientational ordering. Self-organization means a number of complex processes related to the spontaneous alignment and aggregation of anisotropic azobenzene chromophores, processes of collective orientation, self-assembling at the interfaces, etc. The initial anisotropy of nonirradiated polymer films is defined by these processes. We found that the azochromophores in $P1$ films prefer in-plane orientation, whereas the preferential alignment of the fragments in $P2$ films is homeotropic. The factors responsible for this difference have not been studied in detail yet.

The intrinsic self-organization of azochromophores also plays a part in the ordering stimulated by the actinic light [15]. The excitation of azochromophores stimulates these processes of self-organization that are slowed down in the glassy state. The contribution of self-organization processes may explain different anisotropies observed in polymers $P1$ and $P2$ on reaching the state of photosaturation. The positive in-plane order, observed in polymer $P1$, is determined by the strong preference of azochromophores to in-plane alignment.

The negative in-plane order induced in polymer $P2$ by the light with $\lambda_{ex}=488$ nm may be explained by assuming the dominating role of the photoreorientation mechanism. Generally, we know from experience that the negative uniaxial anisotropy with the optical axis parallel to the polarization vector of the exciting light can be easily induced in polymers showing preference to out-of-plane alignment of azochromophores.

The photosaturated state of polymer $P2$ films irradiated at $\lambda_{ex}=365$ nm is found to be optically isotropic with $n_x=n_y=n_z$. As we have already noted in Sec. III B 2, extremely low concentration of *trans* chromophores will render the film effectively isotropic. This is the case even if the angular distribution of *trans* isomers retains an amount of anisotropy caused by the angular selective character of the burning process. On the other hand, nonmesogenic *cis* isomers at high concentrations could result in disordering effects up to suppressing LC properties of azopolymers [45]. From our optical measurements, we cannot unambiguously conclude on the significance of these effects for polymer $P2$.

Thus, in the regime of photoreorientation, the orientational structures observed in the photosaturation state are uniaxial with optical axes determined by the polarization of the light and by the favored orientation of the azochromophores. In the case of photoselection, these structures are optically isotropic. The anisotropic structures induced at the early stages of irradiation are biaxial. These transient structures are formed in passing from the initial uniaxial structure to the state of photosaturation.

Self-organization of azochromophores under irradiation implies their collective orientation and liquid crystallinity. The other collective mode is related to the orientation of nonphotosensitive fragments (matrix), which is influenced by the orientation of azochromophores. According to Refs. [14,24], the latter factor seems to be of crucial importance in stabilizing the photoinduced order.

In our experiments, the photoinduced anisotropy has been seen to be stable over at least several weeks. The anisotropy can be erased and rewritten by the light. This long term stability of the induced order implies effective orientation of polymer matrix in both photoreorientation and photoselection regimes of POA.

In order to interpret the experimental results on the kinetics of the photoinduced absorption dichroism, we employed the theoretical model formulated by using the phenomenological approach of Refs. [18,31]. This approach describes the kinetics of POA in terms of one-particle angular distribution functions and angular redistribution probabilities. The probabilities enter the photoisomerization rates and define coupling between the azochromophores and the anisotropic field represented by the distribution function of the polymer matrix f_p. This anisotropic field reflects the presence of long-living angular correlations and stabilizes the photoinduced anisotropy.

The key assumption of the model is that the *cis* fragments are isotropic and do not affect the ordering kinetics directly. Certainly, this is the simplest case to start from before studying more complicated models. So, we studied the predictions of this simple model for both polymers to test its applicability. To this end, we have estimated a number of photochemical parameters that enter the model from the experimental data. Only the absorption anisotropy parameters and the quantum yields need to be adjusted. The comparison between the numerical results and the experimental data shows that the model correctly captures the basic features of POA in azopolymers.

We have additionally calculated the out-of-plane absorbance D_z and the absorption order parameters $S_i^{(a)}$ in the photoselection regime where the experimental method of estimation is inapplicable. The model has also been applied to estimate concentrations of isomers, quantum yields of photoisomerization, and anisotropy of molecular absorption. It provides a criterion for the occurrence of different mechanisms and describes the biaxiality effects.

So, we have demonstrated that the phenomenological approach of Refs. [18,31] can be used as a useful tool for studying photoinduced ordering processes in azopolymers. But it should be noted that theoretical approaches of this sort, by definition, do not involve explicit considerations of microscopic details of azopolymer physics. A more comprehensive study is required to relate the effective parameters of our model and physical parameters characterizing interactions between molecular units of polymers. For example, the initial anisotropy of polymer films is taken into account through the initial conditions for the kinetic equations and the theory then properly describes the biaxiality effects. But the process of structure formation in nonirradiated polymer films is well beyond the scope of the model and such description cannot serve as an explanation of biaxiality. Similarly, the suppressed out-of-plane reorientation of azochromophores in polymer $P1$ is treated as a constraint imposed by the polymeric environment and is taken into consideration by modifying the order parameter correlation functions.

Our results show that neglecting the influence of *cis* isomers on the orientational order of the anisotropic *trans* isomers does not lead to considerable discrepancies between the theoretical results and the experimental data. In general, the presence of nonmesogenic *cis* isomers could give rise to deterioration of the photoinduced order of *trans* fragments. In the regime of photoselection, this effect will eventually produce nearly isotropic angular distribution of *trans* isomers. On the other hand, our model predicts that in polymer $P2$ this distribution is always anisotropic with nonvanishing order parameters of *trans* fragments. [In this case, the order parameters are not proportional to $S_i^{(a)}$ depicted in Fig. 7(c), which go to zero due to depletion of the *trans* state.] Though the model is successful in describing our experiments, it can be modified to study the case in which the disordering effect caused by *cis* isomers cannot be disregarded.

ACKNOWLEDGMENTS

This study was partially supported by CRDF (Grant No. UP1-2121B). We also thank Dr. T. Sergan from Kent State University for assistance with processing the data of the null ellipsometry measurements and for fruitful discussion.

[1] F. Weigert, Verh. Dtsch. Phys. Ges. **21**, 485 (1919).
[2] B.S. Neporent and O.V. Stolbova, Opt. Spektrosk. **14**, 624 (1963) (in Russian).
[3] T. Todorov, N. Tomova, and L. Nikolova, Appl. Opt. **23**, 4309 (1984).
[4] M. Eich, J.H. Wendorff, B. Reck, and H. Ringsdorf, Makromol. Chem., Rapid Commun. **8**, 59 (1987).
[5] A. Natansohn, S. Xie, and P. Rochon, Macromolecules **25**, 5531 (1992).
[6] N.C.R. Holme, P.S. Ramanujam, and S. Hvilsted, Appl. Opt. **35**, 4622 (1996).
[7] A. Petry, S. Kummer, H. Anneser, F. Feiner, and C. Bräuchle, Ber. Bunsenges. Phys. Chem. **97**, 1281 (1993).
[8] U. Wiesner, N. Reynolds, C. Boeffel, and H.W. Spiess, Liq. Cryst. **11**, 251 (1992).
[9] L. Blinov, M. Kozlovsky, M. Ozaki, K. Skarp, and K. Yoshino, J. Appl. Phys. **84**, 3860 (1998).
[10] O. Yaroshchuk, T. Sergan, J. Lindau, S.N. Lee, J. Kelly, and L.-C. Chien, J. Chem. Phys. **114**, 5330 (2001).
[11] L.M. Blinov and V.G. Chigrinov, *Electrooptic Effects in Liquid Crystal Materials* (Springer-Verlag, Berlin, 1994).
[12] M. Dumont and Z. Sekkat, Proc. SPIE **1774**, 188 (1992).
[13] M. Dumont, S. Hosotte, G. Froc, and Z. Sekkat, Proc. SPIE **2042**, 2 (1994).
[14] G.A. Puchkovs'ka, V.Y. Reshetnyak, A.G. Tereshchenko, O.V. Yaroshchuk, and J. Lindau, Mol. Cryst. Liq. Cryst. **321**, 31 (1998).
[15] Y. Zakrevskyy, O. Yaroshchuk, J. Stumpe, J. Lindau, T. Sergan, and J. Kelly, Mol. Cryst. Liq. Cryst. **365**, 415 (2001).
[16] T. Buffeteau and M. Pézolet, Macromolecules **31**, 2631 (1998).
[17] A. Kiselev, O. Yaroshchuk, Y. Zakrevskyy, and A. Tereshchenko, Condens. Matter Phys. **4**, 67 (2001).
[18] O. Yaroshchuk, A.D. Kiselev, Y. Zakrevskyy, J. Stumpe, and J. Lindau, Eur. Phys. J. E **6**, 57 (2001).
[19] S. Hvilsted, F. Andruzzi, and P.S. Ramanujam, Opt. Lett. **17**, 1234 (1992).
[20] A. Natansohn, P. Rochon, X. Meng, C. Barett, T. Buffeteau, S. Bonenfant, and M. Pezolet, Macromolecules **31**, 1155 (1998).
[21] T. Fisher, L. Läsker, J. Stumpe, and S.G. Kostromin, J. Photochem. Photobiol., A **80**, 453 (1994).
[22] T.G. Pedersen and P.M. Michael, Phys. Rev. Lett. **79**, 2470 (1997).
[23] T.G. Pedersen, P.M. Johansen, N.C.R. Holme, P.S. Ramanujam, and S. Hvilsted, J. Opt. Soc. Am. B **15**, 1120 (1998).
[24] O.V. Yaroshchuk, V.Y. Reshetnyak, A.G. Tereshchenko, L.I. Shans'ky, G.A. Puchkovs'ka, and J. Lindau, Mater. Sci. Eng., C **C8–C9**, 211 (1999).
[25] T.A. Sergan, S.H. Jamal, and J.R. Kelly, Displays **20**, 259 (1999).
[26] A. Dyadyusha, A. Khizhnyak, T. Marusii, Y. Reznikov, O. Yaroshchuk, V. Reshetnyak, W. Park, S. Kwon, and D. Kang, Mol. Cryst. Liq. Cryst. **263**, 399 (1995).
[27] L.M. Blinov, N.V. Dubinin, V.G. Rumyancev, and S.G. Yudin, Opt. Spektrosk. **55**, 679 (1983) (in Russian).
[28] A. Osman and M. Dumont, Opt. Commun. **164**, 277 (1999).
[29] W. Feng, S. Lin, B. Hooker, and A. Mickelson, Appl. Opt. **34**, 6885 (1995).
[30] V. Cimrova, D. Neher, S. Kostromine, and T. Bieringer, Macromolecules **32**, 8496 (1999).
[31] A.D. Kiselev, J. Phys.: Condens. Matter **14**, 13417 (2002).
[32] A. Böhme, E. Novotna, H. Kresse, F. Kuschel, and J. Lindau, Macromol. Chem. Phys. **194**, 3341 (1993).
[33] O. Yaroshchuk, D.M. Agra, Y. Zakrevskyy, L.-C. Chien, J. Lindau, and S. Kumar, Liq. Cryst. **28**, 703 (2001).
[34] *Ellipsometry and Polarized Light*, edited by R.M.A. Azzam and N.M. Bashara (North-Holland, Amsterdam, 1977).
[35] D.W. Berreman, J. Opt. Soc. Am. **62**, 502 (1972).
[36] M. Phaadt, C. Boeffel, and H.W. Spiess, Acta Polym. **47**, 35 (1996).
[37] C.S. Paik and H. Morawets, Macromolecules **5**, 171 (1972).
[38] C. Eisenbach, Ber. Bunsenges. Phys. Chem. **84**, 680 (1980).
[39] I.Y. Bernstein and Y.L. Kaminskii, *Spectrophotometric Analysis in Organic Chemistry* (Khimiya, Leningrad, 1975) (in Russian).
[40] S. Sajti, A. Kerekes, M. Barabás, E. Lörincz, S. Hvilsted, and P.S. Ramanujam, Opt. Commun. **194**, 435 (2001).
[41] M. Dumont, in *Photoactive Organic Materials*, edited by F. Kajzar *et al.* (Kluwer Academic, The Netherlands, 1996), pp. 501–511.
[42] P.G. de Gennes and J. Prost, *The Physics of Liquid Crystals* (Clarendon Press, Oxford, 1993).
[43] P.M. Chaikin and T.C. Lubensky, *Principles of Condensed Matter Physics* (Cambridge University Press, Cambridge, 1995).
[44] I. Mita, K. Horie, and K. Hirao, Macromolecules **22**, 558 (1989).
[45] A. Kanazawa, S. Hirano, A. Shido, M. Hasegawa, O. Tsutsumi, T. Shiono, T. Ikeda, Y. Nagase, E. Ikiyama, and Y. Takamura, Liq. Cryst. **23**, 293 (1997).